Motion Model of Bench Dragon Based on The Spiral Algorithm

Hongyu Li [1, #], Jiahua Wang [2, #], Zhiyi Chen [1, *, #]

[1] College of National Defense Science and Technology, Southwest University of Science and Technology, Mianyang, China, 621010

[2] College of Information Engineering, Southwest University of Science and Technology, Mianyang, China, 621010

* Corresponding Author Email: 17759088587@163.com

[#]These authors contributed equally.

Abstract. This study focuses on the potential collision scenarios in the motion of the Bench Dragon, a traditional folk activity, aiming to precisely locate possible collision points. Currently, there is a dearth of specialized research and experimental exploration on bench dragon collisions. By leveraging the known spiral equation and triangular relationships, the study first deduces the motion correlations among benches to accurately ascertain their positions and velocities. Then, through simulating the motion of two benches, it clarifies the collision-triggering conditions. To boost solution efficiency, a nearest-neighbor detection model for adjacent layers is proposed. A subsequent simulation analysis of the bench dragon's overall motion reveals that at the 412.3rd second, the dragon's head will collide with the 8th section of its body. The results validate the model, filling the research gap and aiding in understanding the dragon's motion and collisions.

Keywords: Archimedean Spiral, Collision Model, Triangle Theorem.

1. Introduction

The excellent traditional Chinese culture is profound and extensive, among which the "Bench Dragon" is a unique folk activity in Zhejiang and Fujian regions, consisting of tens to hundreds of benches connected together[1]. When forming the dragon, the head leads the body and tail to wind around, and then unwinds from the tail. The appreciation value lies in the small area and high speed of the dragon's winding. To reduce the time complexity of solving collision points, Gottschalk et al. proposed the RAPID algorithm, significantly improving the efficiency of the solution. Based on the RAPID algorithm[2], Lin Fei et al. in their optimized collision detection algorithm based on composite hierarchical bounding boxes, further improved the solution efficiency by selecting separation axes in different ways according to the hierarchy of the bounding box nodes, thereby reducing the number of separation axis tests in the intersection detection process and enhancing detection efficiency[3]. Xu Mingkai et al, in "Spatiotemporal Correlation in Multi-object Collision Detection" [4], addressed the limitation of spatiotemporal correlation algorithms in detecting only two-object collisions by proposing an improved algorithm that combines spatial region division and temporal correlation to solve the multi-object collision problem and ensure effectiveness at high speeds. Ye Jiaxuan, in the multi-body separation simulation method including object collisions, proposed a numerical simulation method for research and analysis to solve the problem that traditional multi-body separation research methods cannot solve collision problems. Despite significant achievements in the field of collision detection by the aforementioned scholars, their conclusions are still inadequate in addressing the potential collisions among multiple benches due to dynamic changes in radial distance and angle during the spiral movement of the Bench Dragon. In view of this, this paper conducts in-depth experimental research. Contributions of this paper: Based on the known spiral equation, this study accurately derives the motion correlations between each bench using triangular relationships, thereby precisely determining the position and velocity of each bench. By simulating the motion states of two benches, this study clarifies the specific conditions for collisions and propose a nearest-neighbor detection model for adjacent layers to improve the efficiency of problem-solving. This paper applies this model to this problem context for the first time and to the research topic of detecting multi-object collisions. In the relevant theoretical sections, this study elaborates on the core principles of the Archimedean spiral, cosine theorem, and nearest-neighbor detection model for adjacent layers. In the experimental sections, this study first obtains the position and velocity information of the benches, then determine the collision conditions and discern the intersection situations. To enhance detection efficiency, this study introduces the nearest-neighbor detection model for adjacent layers. Subsequently, this study constructs a model to solve the real-time positions and velocities of the dragon's head and any bench, and based on this, this study judges the collision situations between two benches and accurately locate the time point of collision. In the conclusion section, this study provides a detailed analysis of the experimental results. In the summary section, this study summarizes the core contributions of this study: proposing a collision detection model based on the spiral algorithm and successfully verifying its effectiveness; clearly pointing out the specific time points of collisions; and envisioning the potential application value of this model in deepening the understanding of [6] the motion characteristics of the Bench Dragon and extending it to other folk activities.

2. Related Theories

Archimedean spiral: The Archimedean spiral has the characteristic of a uniform spiral, which means that as a moving point moves at a constant speed along a straight line, the line simultaneously rotates around a point on it at a constant angular velocity. The path traced by the moving point is the Archimedean spiral.

1)Expressed in polar coordinates, the equation is:

$$\rho = a\theta \tag{1}$$

Where ρ represents the radial distance, θ represents the polar angle a is a constant, representing the starting radius of the spiral or the ratio of the initial speed to the angular velocity.

2)In Cartesian coordinates, the equation is expressed as:

$$r = a + b\theta \tag{2}$$

Where $r$represents the distance from the point to the origin, θ is the angular variable, a and b are constants.

Cosine Theorem: The Cosine Theorem is a mathematical theorem that describes the relationship between the square of one side of a triangle and the sum of the squares of the other two sides minus twice the product of these two sides and the cosine of the angle between them[5].

The specific statement of the Cosine Theorem is: For any triangle $\triangle ABC$, if a , b and c represent the lengths of the three sides of the triangle, and $\angle A$, $\angle B$ and $\angle C$ are the corresponding angles, then the following relationship holds:

$$c^2 = a^2 + b^2 - 2abcos\angle c \tag{3}$$

The specific triangle is shown in Figure 1.

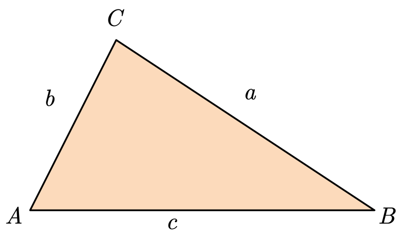

Figure 1. iagram of Triangle abc

Nearest Neighbor Detection Model for Adjacent Layers: To address the time complexity arising from collision detection in the bench dragon, this study proposes starting from the lead bench and drawing lines connecting the front and rear handles to the center of the spiral. this study then extend these lines to intersect their adjacent layers at two points, calculate the polar angles of these two points, and identify three benches with polar angles close to those of these two points for collision detection. The specific process is shown in Figure 2 below:

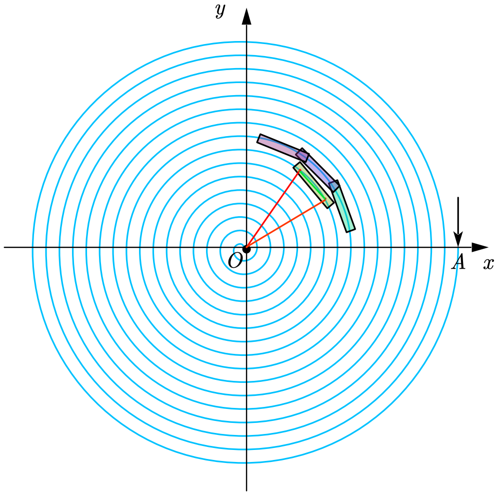

Figure 2. Diagram of Collision Detection for Adjacent Layers

3. Experiment

Firstly, this study obtains the position and velocity of the benches at any given time through geometric relationships. Next, this study confirms the collision conditions by establishing a univariate linear equation for the two benches. Through geometric relationships, this study derives the edge function of the benches and determine whether there are intersection points between the edges of the two benches by limiting the range of the independent variable for the bench edges. If there are intersection points, a collision occurs; otherwise, there is no collision. Finally, to improve the efficiency of the judgment, this study starts from the lead bench, draw lines connecting the front and rear handles to the center of the spiral, and extend these lines to intersect their adjacent layers at two points. this study then calculates the polar angles of these two points and identify three benches with polar angles close to those of these two points for collision detection.The specific flowchart is shown in Figure 3.

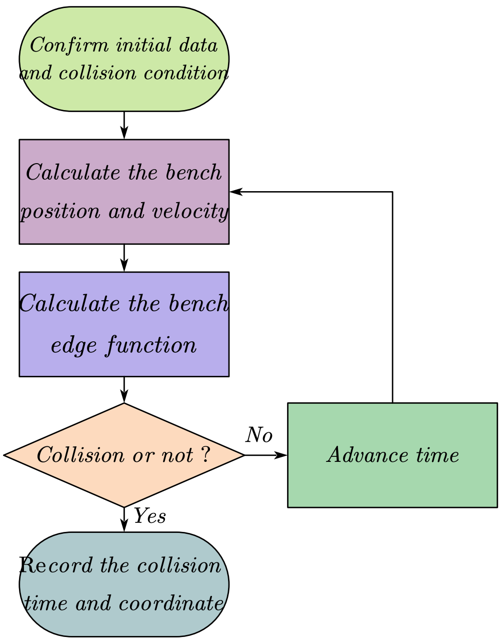

Figure 3. Flowchart of the Bench Dragon Collision Experiment

3.1. Solution for the position and velocity of the front handle of the leading bench

Taking the front handle of the leading bench as the reference point, it performs a spiraling motion. Assuming that after a period of time, the arc length traveled by the front handle of the leading bench is:

$$S = vt \tag{4}$$

Where S is the arc length and v is the velocity of the front handle of the leading bench. Based on the integral of the arc:

$$S = \int_0^{\theta} \rho(\theta) d\theta \approx \rho(\theta) \cdot \theta \tag{5}$$

Through formulas (4) and (5), the relationship between the angle of the front handle of the leading bench and time is obtained as:

$$t = \frac{\rho(\theta) \cdot \theta}{v} \tag{6}$$

Given in $\rho(\theta)$, substituting it into formula (5) and simplifying, this study gets:

$$\frac{p}{2\pi}\theta^2 + \rho_0\theta - vt = 0 \tag{7}$$

This is a quadratic equation about θ Solving for it, this study gets:

$$\theta(t) = \frac{-\rho_0 \pm \sqrt{-\rho_0 + \frac{2p}{\pi}vt}}{\frac{p}{\pi}} \tag{8}$$

Where p is the pitch. Since the angle is positive, so let the answer (9) omit:

$$\theta(t) = \frac{-\rho_0 - \sqrt{-\rho_0 + \frac{2p}{\pi}vt}}{\frac{p}{\pi}} \tag{9}$$

In this study, by substituting the function in which the angle varies with time into the helical equation, the relationship between the polar radius of the front handle of the faucet and time can be obtained as follows:

$$\rho(t) = \rho_0 + \frac{p \cdot \theta(t)}{2\pi} \tag{10}$$

Convert the polar coordinates of the front handle into two-dimensional Cartesian coordinates:

$$\begin{cases} x = \rho(t) \cdot cos\theta(t) \\ y = \rho(t) \cdot sin\theta(t) \end{cases} \tag{11}$$

During the winding process, the velocity of the faucet's front handle is decomposed along the tangential and radial directions, where the tangential velocity components along the xy-axis are:

$$\begin{cases} v_{\theta x} = v \cdot cos(90^\circ - \theta) \\ v_{\theta y} = v \cdot sin(90^\circ - \theta) \end{cases} \tag{12}$$

The components of the radial velocity along the xy-axis are:

$$\begin{cases} v_{rx} = \frac{dr(t)}{dt} \cdot cos\theta(t) \\ v_{ry} = \frac{dr(t)}{dt} \cdot sin\theta(t) \end{cases} \tag{13}$$

According to the principle of superposition, the velocity of the faucet's front handle along the xy direction is:

$$\begin{cases} v_x = v \cdot cos(90^\circ - \theta) + \frac{dr(t)}{dt} \cdot cos\theta(t) \\ v_y = v \cdot sin(90^\circ - \theta) + \frac{dr(t)}{dt} \cdot sin\theta(t) \end{cases} \tag{14}$$

3.2. The position and velocity calculation for the rear handle of the faucet

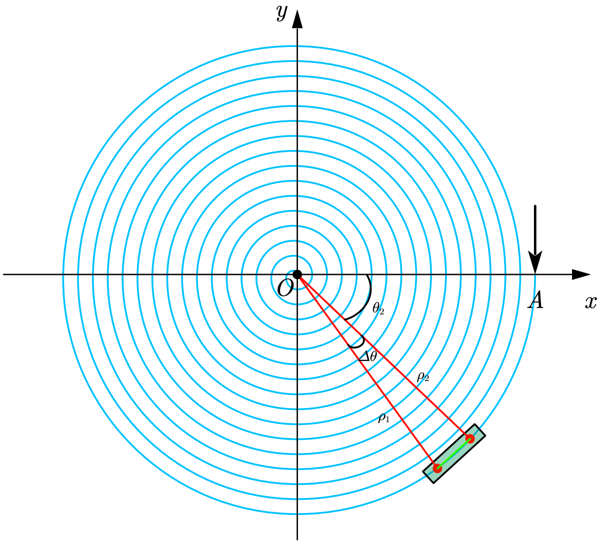

Figure 4. Schematic Diagram of the Positions of the Front and Rear Handles of the Faucet

As shown in the figure 4 above, during the winding process, there are the angle difference $\Delta\theta$ between the front and rear handles of the faucet, the distance ρ_1 from the center of the helix to the front handle, the distance ρ_2 from the center of the helix to the rear handle, and the distance l_1 between the front and rear handles of the faucet.

Based on the known conditions mentioned above[6], according to the cosine theorem, this study has:

$$l_1^2 = \rho_1^2 + \rho_2^2 - 2\rho_1\rho_2 cos\Delta\theta \tag{15}$$

Where $\rho_1 = \rho_0 + \frac{p\theta_1}{2\pi}$, $\rho_2 = \rho_0 + \frac{p\theta_2}{2\pi}$. Substituting ρ_1 , ρ_2 into the above equation, this study gets:

$$l_1^2 = (\rho_0 + \frac{p\theta_1}{2\pi})^2 + (\rho_0 + \frac{p\theta_2}{2\pi})^2 - 2(\rho_0 + \frac{p\theta_1}{2\pi})(\rho_0 + \frac{p\theta_2}{2\pi})cos\Delta\theta \tag{16}$$

Since $\Delta\theta = \theta_1 - \theta_2$, this study replaces θ_2 with $\theta_1 - \Delta\theta$. Solving the equation, this study obtains $\Delta\theta = \theta_1 - \theta_2$, $\theta_2 = \theta_1 - \Delta\theta$. Then the position at the next moment is:

$$\begin{cases} x_2 = \rho_2(t) \cdot cos\theta_2(t) \\ y_2 = \rho_2(t) \cdot sin\theta_2(t) \end{cases} \tag{17}$$

After solving for the polar radius, the components of the velocity of the rear handle of the faucet along the xy-axis can be determined using the following formulas:

$$\begin{cases} v_{x2} = \frac{dx_2}{dt} = \frac{d(\rho_2 \cdot cos\theta_2(t))}{dt} \\ v_{y2} = \frac{dy_2}{dt} = \frac{d(\rho_2 \cdot sin\theta_2(t))}{dt} \end{cases} \tag{18}$$

Therefore, this study can recursively deduce the position and velocity of the i bench at any time t as:

$$\begin{cases} x_2 = \rho_2(t) \cdot cos\theta_2(t) \\ y_2 = \rho_2(t) \cdot sin\theta_2(t) \\ v_{x2} = \frac{dx_2}{dt} = \frac{d(\rho_2 \cdot cos\theta_2(t))}{dt} \\ v_{y2} = \frac{dy_2}{dt} = \frac{d(\rho_2 \cdot sin\theta_2(t))}{dt} \end{cases} \tag{19}$$

3.3. The definition of collision

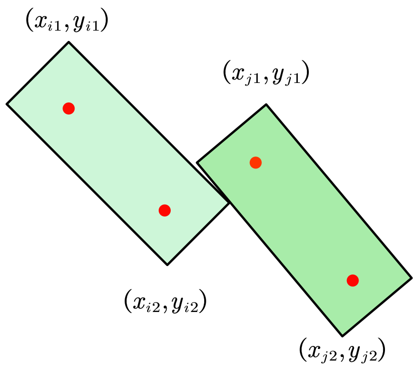

Figure 5. Diagram of Two Benches Colliding

The collision schematic is shown in Figure 5. Based on equation set (19), this study can obtain the position of the i handle of any bench. To determine whether a collision occurs between two benches[7], this study needs to establish a unary function using the coordinates of the front and rear handles of the inner bench:

$$y = \frac{y_{i1} - y_{i2}}{x_{i1} - x_{i2}} \cdot (x - x_{i1}) \tag{20}$$

Based on the parallel relationship between the line connecting the front and rear handles and the long edge of the bench[8], this study can obtain a unary linear function for the long edge of the inner bench that is closest to the outer circle:

$$y = \frac{y_{i1} - y_{i2}}{x_{i1} - x_{i2}} \cdot (x - x_{i1}) + \frac{d}{2} \tag{21}$$

Where d is the width of the bench.

The unary function for the inner long edge of the outer bench j is:

$$y = \frac{y_{j1} - y_{j2}}{x_{j1} - x_{j2}} \cdot (x - x_{j1}) - \frac{d}{2} \tag{22}$$

By solving the linear functions of the long edges of the inner bench i and the outer bench j simultaneously, this study obtains the following:

$$\begin{cases} y = \frac{y_{i1} - y_{i2}}{x_{i1} - x_{i2}} \cdot (x - x_{i1}) + \frac{d}{2} \\ y = \frac{y_{j1} - y_{j2}}{x_{j1} - x_{j2}} \cdot (x - x_{j1}) - \frac{d}{2} \end{cases} \tag{23}$$

If there are no intersection points, then the benches do not collide; if there are intersection points, then the coordinates of the intersection points are (x_0, y_0) , and the benches may collide. The following is a discussion on whether the intersection point (x_0, y_0) is a collision point.

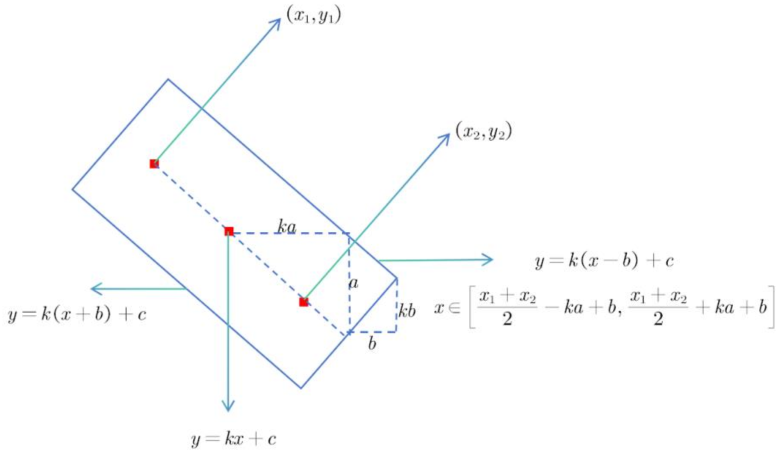

Figure 6. Neighborhood of the outer long edge of the inner bench

From the above figure 6, this study can derive the x-neighborhood of the inner bench i as:

$$(\frac{x_{i1}+x_{i2}}{2} - kb + a, \frac{y_{i1}+y_{i2}}{2} + kb + a) \tag{24}$$

Where:

$$\begin{cases} b^2 + (kb)^2 = (\frac{l}{2})^2 \\ a^2 + (ka)^2 = (\frac{d}{2})^2 \end{cases} \tag{25}$$

l is the length of the bench, d is the width of the bench, and k is the slope of the unary linear function.

From the above solution process, it can be seen that if the coordinate (x_0, y_0) of the intersection point is within the x-neighborhood of the outer long edge of the inner bench, then the benches collide.

3.4. Check for collision

Having clarified the conditions for collision, in order to investigate the potential collisions between the dragon's head, body, and tail after 300 seconds, this study continues the movement with a step size of $\Delta t = 0.01s$. After each movement, this study starts from the inner layer of benches, which represent the dragon's head, and check whether it collides with any other benches. If no collision occurs, the movement continues until the first point in time when a collision occurs is found.

In practical calculations, starting from the inner layer of benches to determine whether they collide with all the outer benches and their would result in significant computational complexity and meaningless results. To simplify the computation, this study proposes a model. By extending the polar radii of the front and rear handles of the inner layer benches, which are determined by their polar angles, until they intersect with the helix of the outer layer adjacent to the inner layer benches, this study obtains the intersection points with polar angles $\theta_{i1} - 2\pi$, $\theta_{i2} - 2\pi$, respectively. After finding these intersection points, this study searches for the three benches closest to these two points. Then, using the conditions for collision [9], this study solves the functions of the long edges of the inner layer bench and the three outer layer benches simultaneously to determine if a collision occurs[10]. This approach ensures that no potentially colliding benches are missed while avoiding excessive computational complexity, thus improving the efficiency of the model solution.

4. Results

Through the experimental derivation mentioned above, this study has obtained the positions and velocities of the benches at any moment when the dragon's head maintains a constant speed of 1m/s.

Due to space limitations, this study only lists the positions and velocities of the dragon's head, the 1st section of the dragon's body, the 51st section of the dragon's body, the 101st section of the dragon's body, the 151st section of the dragon's body, the 201st section of the dragon's body, and the dragon's tail at 0s, 60s, 120s, 180s, 240s, and 300s. The details are shown in Table 1, Table 2 below:

Table.1. Positions of the Bench Dragon at Special Moments

	0 s	60 s	120 s	180 s	240 s	300 s
The x of the dragon's head (m)	8.8	5.79727	-4.090058	-2.954498	2.58081	4.430259
The y of the dragon's head (m)	0	-5.773149	-6.301179	6.0992	-5.363265	2.300853
The x of the 1st section of the dragon body (m)	8.379861	7.417462	-1.541262	-5.167956	4.762495	2.556146
The y of the 1st section of the dragon body (m)	2.776997	-3.522068	-7.385381	4.439314	-3.637788	4.3448
The x of the 51st section of the dragon body (m)	-8.775627	-7.351903	-2.802937	5.492665	3.520091	-4.915833
The y of the 51st section of the dragon body (m)	3.864116	5.227435	7.936818	5.494022	-6.117778	3.886244
The x of the 101st section of the dragon body (m)	-2.032804	0.467909	-0.232941	-3.981159	-7.958326	-0.25854
The y of the 101st section of the dragon body (m)	-10.092414	-9.75548	-9.20734	-7.646111	-0.61041	7.286019
The x of the 151st section of the dragon body (m)	9.491345	10.402646	8.946819	8.305111	8.723996	6.420019
The y of the 151st section of the dragon body (m)	-5.468984	1.085218	4.329801	4.386903	1.24518	-5.087381
The x of the 201st section of the dragon body (m)	11.078808	3.071524	-4.006095	-7.542614	-7.992463	-6.042669
The y of the 201st section of the dragon body (m)	3.355266	10.680085	9.836887	6.7339	5.270804	6.672382
The x of the dragon's tail (m)	-11.20492	-2.615236	6.653226	10.018273	9.900328	9.344407
The y of the dragon's tail (m)	-3.869049	-11.087981	-8.658965	-2.885189	0.053486	-0.247454

The following Table 2 shows the velocities at special positions.

Table.2. Velocities of the "Bench Dragon" at Special Moments

	0 s	60 s	120 s	180 s	240 s	300 s
dragon head (m/s)	1	1	1	1	1	1
The 1st section of the dragon body (m/s)	0.999936	0.999928	0.999914	0.999895	0.999863	0.999805
The 51st section of the dragon body (m/s)	0.998285	0.998049	0.997728	0.997273	0.996596	0.995463
The 101st section of the dragon body (m/s)	0.996867	0.996464	0.995932	0.9952	0.994148	0.992454
The 151st section of the dragon body (m/s)	0.99563	0.9951	0.994416	0.993494	0.992182	0.990144
The 201st section of the dragon body (m/s)	0.994532	0.993894	0.993097	0.99203	0.990538	0.988278
The dragon's tail (m/s)	0.994059	0.993401	0.992547	0.991423	0.989874	0.987533

Figure 7 is a schematic diagram of the bench dragon's movement at 60s and 240s.

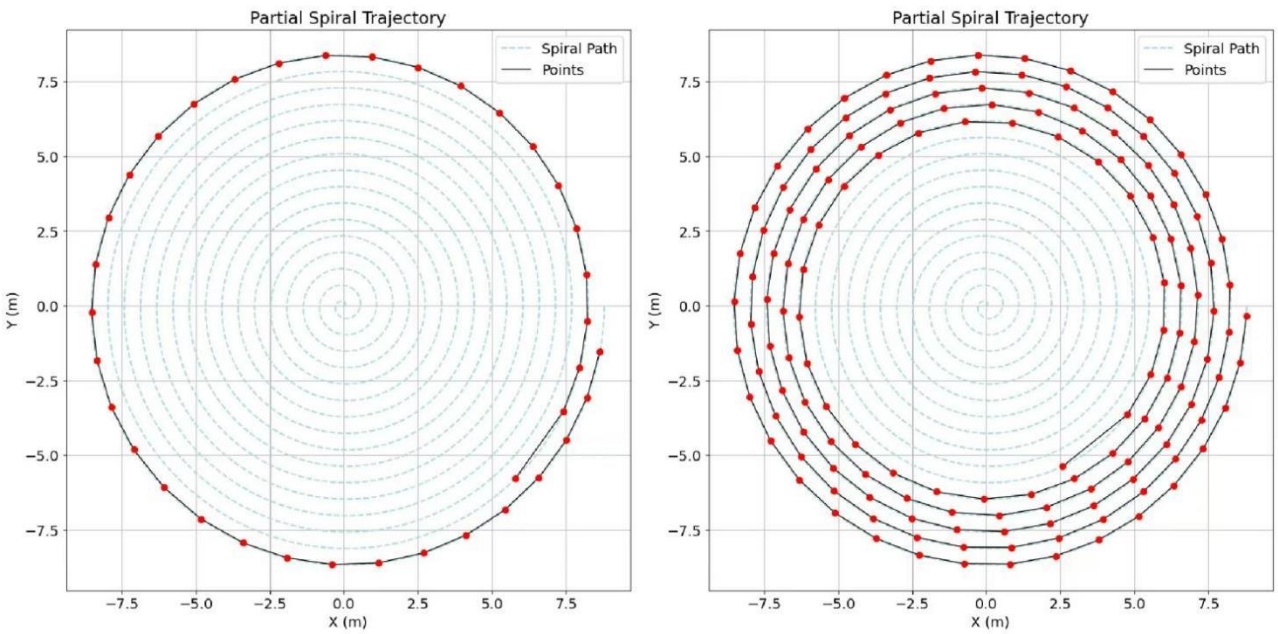

Figure 7. Movement position diagram at 60s and 240s

Based on the above results, this study can draw the following conclusions:

The speed of each handle is basically consistent with the fixed speed of the dragon head. Analyzing the speeds of the 1st and 51st sections of the dragon body at 120s, the difference is only 0.0022m/s. Analyzing the speeds of different sections of the dragon body at different times, there is basically no difference. The reason for this may be that the bench is a rigid body and does not deform by itself. If there were a significant speed difference, it could potentially lead to the bench breaking.

Due to the decreasing polar radius of the spiral, collisions may occur between the boards. After continuously simulating the movement of the "bench dragon" beyond 300 seconds, it was found that the dragon head might collide with other parts of the dragon body when approaching the center of the spiral.

Through experimental derivation to detect the occurrence of collisions, this study obtained the positions and velocities of each bench one second before the collision. Similarly, to reduce the length of the text, this study still selects the positions and velocities of specific benches at specific times. The results obtained are as Table 3 follows:

Table.3. Position and Velocity Table of the "Bench Dragon" at the Moment of Collision

	x (m)	y (m)	v (m/s)
dragon head	1.020734	2.058396	1
The 1st section of the dragon body	1.726441	1.677928	0.999066
The 51st section of the dragon body	4.13592	1.593249	0.986945
The 101st section of the dragon body	-5.737726	-0.748613	0.981697
The 151st section of the dragon body	6.862909	-0.504428	0.9783
The 201st section of the dragon body	0.876468	7.778454	0.975782
The dragon's tail	7.869913	-2.387917	0.974818

The schematic diagram of the collision moment is shown in Figure 8.

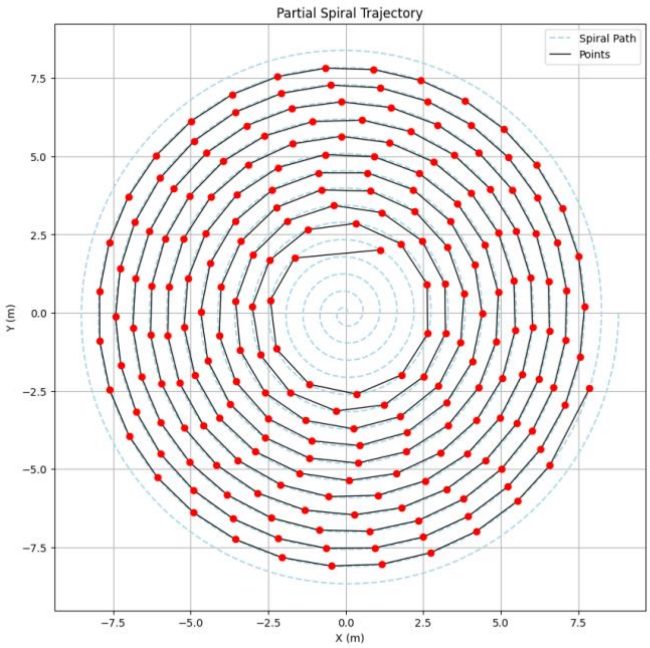

Figure 8. Position Diagram at the Moment of Collision

Based on the above research, the analysis of the results is as follows:

Due to the decrease in polar radius and the significant change in polar angle per unit time near the center of the spiral, collisions are likely to occur. Since the dragon head is longer than the dragon body and initiates the spiral movement first, when a collision occurs at 412.3 seconds, only the dragon head collides with other parts of the dragon body.

5. Conclusions

In this paper,this study conducted an in-depth study on the potential collision problems during the movement of the "Bench Dragon" based on the spiral algorithm. Using the known spiral equation, this study accurately derived the motion correlations between each bench through trigonometric relationships, thereby precisely determining the position and velocity of each bench. Next, this study simulated the movement states of two benches, clarified the specific conditions for collisions to occur, and proposed a nearest neighbor detection model for adjacent layers to improve the efficiency of the solution.

Through simulation and analysis, this study found that at the 412.3rd second, the dragon head will collide with the 8th section of the dragon body, although the specific coordinates of the collision point were not detailed in the paper. This result verifies the correctness and effectiveness of the collision model this study proposed, filling a gap in current research.

The model this study proposed not only provides important support for a deeper understanding of the movement characteristics and collision situations of the "Bench Dragon", but also holds promise for future extension to collision detection in other similar folk activities, offering new ideas and methods for solving related problems.

References

[1] Li Moutao. Adhering to the Tradition and Innovating: An Oral History Investigation Based on the Inheritors of the Intangible Cultural Heritage "Huizhou Bench Dragon" [J]. Journal of Tonghua Normal University, 2024, 45(3): 31-37.

[2] Zhao Di, Wang Xiongjin, Chen Guo, et al. An Adaptive Bounding Box Collision Detection Method Based on Approximate Convex Hull [J]. Science Technology and Engineering, 2023, 23(22): 9592-9598.

[3] Lin Fei, Zou Ling, Zhang Cong. A Fast Collision Detection Algorithm Based on Hybrid Hierarchical Bounding Boxes [J]. Computer Simulation, 2023, 40(9): 454-457.

[4] Yan Juntuan, Pei Yanan, Yao Hong, et al. Collision Detection Based on Fruit Fly Optimization Algorithm in Virtual Reality [J]. Journal of Nanjing University of Science and Technology, 2023, 47(1): 74-80.

[5] He Ting, Wu Yanqiu, Feng Jiao. Teaching Design of Cosine Theorem Based on Core Competency Cultivation [J]. Sanxia Journal of Higher Education Research, 2023(2): 44-50.

[6] Gao Shuangyun. The Application of Trigonometric Functions in Physical Motion Problems [J]. Mathematics and Physics World: High School Edition, 2023(21): 97-97.

[7] Ma Baoxing. Mathematics Teaching in the Context of "Big Ideas" - Taking the Yan Juntuan, Pei Yanan, Yao Hong, et al. Collision Detection Based on Fruit Fly Optimization Algorithm in Virtual Reality [J]. Journal of Nanjing University of Science and Technology, 2023, 47(1): 74-80.

[8] Yan Juntuan, Pei Yanan, Yao Hong, et al. Collision Detection Based on Fruit Fly Optimization Algorithm in Virtual Reality [J]. Journal of Nanjing University of Science and Technology, 2023, 47(1): 74-80.

[9] Li Moutao. Keeping the Right Course and Making Innovations: An Investigation Based on the Oral History of the Inheritors of the Intangible Cultural Heritage "Huizhou Bench Dragon" [J]. Journal of Tonghua Normal University, 2024, 45(3): 31-37.

[10] Sun Jieni. Research on the Communication Strategies of Datian Bench Dragon [J]. Masterpieces of Nature, 2024(18): 54-56.